IEEE Photonics Journal
An IEEE Photonics Society Publication

Open Access

OAM-Based Hybrid Free-Space Optical-Terahertz Multidimensional Coded Modulation and Physical-Layer Security

Volume 9, Number 4, August 2017

Ivan B. Djordjevic

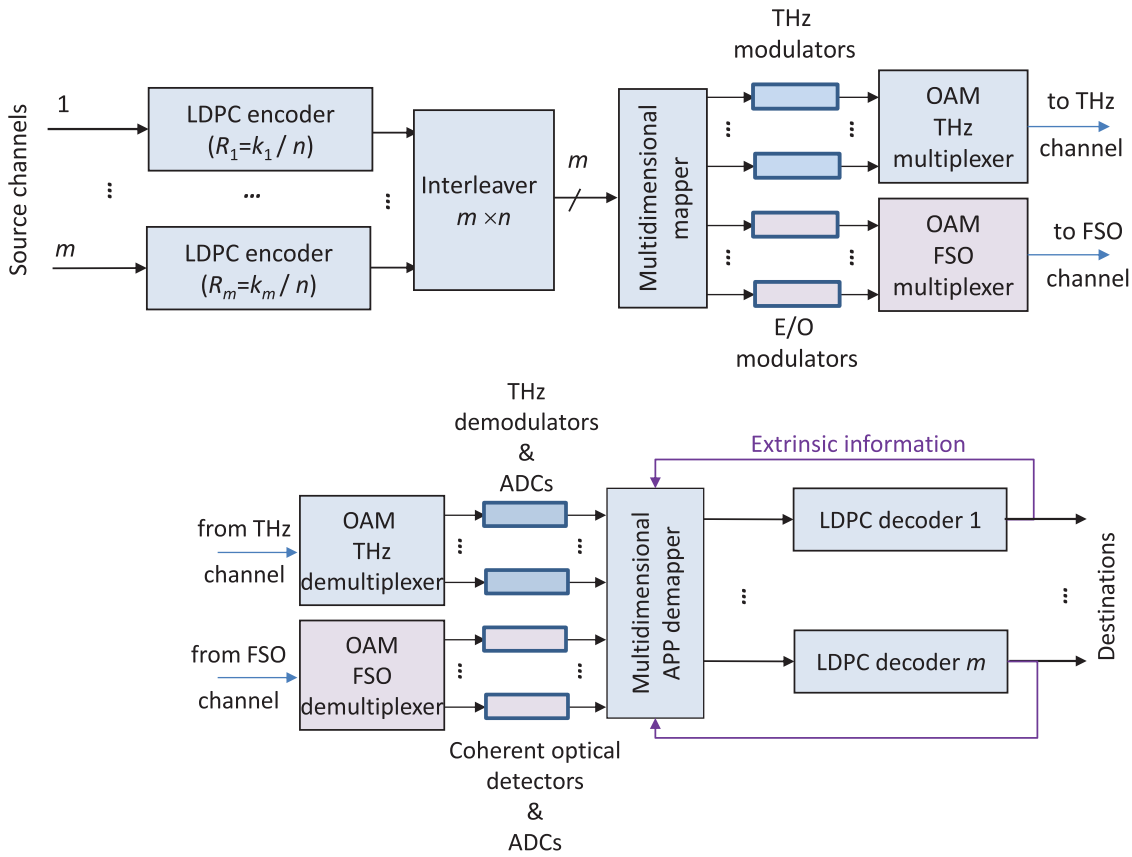

DOI: 10.1109/JPHOT.2017.2724563
1943-0655

OAM-Based Hybrid Free-Space Optical-Terahertz Multidimensional Coded Modulation and Physical-Layer Security

Ivan B. Djordjevic

Department of Electrical and Computer Engineering, University of Arizona, Tucson, AZ 85721 USA

DOI:10.1109/JPHOT.2017.2724563

Manuscript received June 28, 2017; accepted July 5, 2017. Date of publication July 11, 2017; date of current version August 14, 2017.

Abstract: To address capacity constraints and physical-layer security (PLS), defined in information-theoretic sense, of both optical and wireless networks in a simultaneous manner, we propose to use the hybrid free-space optical (FSO)-THz technologies employing orbital angular momentum (OAM) modes in both FSO and THz subsystems. The OAM modes, related to azimuthal dependence of the wavefront, are mutually orthogonal so that this additional degree of freedom can be utilized to improve both spectral efficiency and PLS in both optical and wireless networks. Spatial light modulators (SLMs) are routinely used to generate OAM modes in optical domain, in particular in FSO communications links. On the other hand, it has been recently demonstrated that a traveling-wave circular loop antenna, with azimuthal phase distribution along the loop, can be used to generate OAM in the RF domain. Reliability of FSO links is affected by atmospheric turbulence effects, scattering effects, and low-visibility in foggy conditions. On the other hand, RF technologies are not affected by these effects, but are sensitive to rain and snow. In particular, THz technologies, have available bandwidths comparable to a typical wavelength channel in WDM systems. Based on this complementarity, here we propose to use hybrid FSO-THz technologies to significantly improve the spectral efficiency and PLS of both FSO and wireless communications systems and networks.

Index Terms: Physical-layer security, orbital angular momentum (OAM), free-space optical (FSO) communication, hybrid FSO-terahertz technology, multidimensional coded modulation, atmospheric turbulence, multipath fading.

1. Introduction

The Internet and data traffic exponential growths place enormous pressure on the underlying information infrastructure at every level, ranging from the core to access networks. As the response to these never-ending data traffic demands ITU-T, IEEE 802.3ba, and OIF have completed the standardization work on 100 Gb/s Ethernet (100 GbE) [1], [2], while the research focus has moved to higher bit rates (400 Gb/s, 1 Tb/s, and beyond). To address optical network capacity constraints, we proposed recently a transformational strategy employing higher degrees of freedom per photon to enable the ultra-high capacity network connections [1]–[3]; including amplitude, phase, frequency, polarization, and orbital angular momentum (OAM). On the other hand, in the wireless domain, key challenges for beyond 5G access technologies include limited wireless bandwidth infrastructure; insufficient energy-, cost-, and resource-efficiencies; heterogeneity of network segments, high traffic demands, the existence of various cell sizes (small cells), interference management, introduction

of intelligence, and security issues. Moreover, the 5G will be user-centric driven instead of service-centric 4G [4]–[8]. We anticipate that beyond 5G networks will provide an open communication platform to integrate cellular systems, satellite systems, data centers, business/home gates, and any future open and cloud networks. The optical access networks to enable the 5G deployment must be scalable to provide at least 1–10 Gb/s at the user terminal, 100 Gb/s for the backhaul, 1 Tb/s for metro, and 1 Pb/s for the core transport [9]. These goals are quite difficult to achieve with currently existing optical networks technologies. It is, therefore, necessary to make a dramatic improvement in both optical and wireless signal transmission rates in order to cope with the incoming bandwidth capacity crunch.

Although there are some proposals on how to deal with the incoming bandwidth capacity crunch [1]–[3], the security of optical networks seems to be almost completely neglected. By taping out the portion of optical signal, the huge amount of data can be compromised. Therefore, the security of future optical and wireless networks is becoming one of the major issues to be addressed sooner rather than later. Thanks to its flexibility, security, immunity to interference, high-beam directivity, and energy-efficiency, the free-space optical (FSO) technology represents an excellent candidate for high-performance secure communications. Despite these advantages, large-scale deployment of FSO systems has been so far affected by reliability and availability issues due to atmospheric turbulence in clear weather, low visibility in foggy conditions, Mie scattering effects, and high sensitivity to misalignment [10]. Because of high directivity of optical beams, the FSO links are much more challenging to intercept compared to RF systems. Nevertheless, the eavesdropper can still apply the beam splitter on transmitter side, the blocking attack, or exploit beam divergence at the receiver side. The research on FSO physical-layer security (PLS) is getting momentum, which can be judged based on increased number of recent papers related to this topic, such as [11], [12]. Most of papers on the physical-layer security for FSO communications are based on direct detection and employ wiretap channel approach introduced by Wyner [13]. The fog represents the most detrimental factor that impacts the reliability of an FSO link. In contrast, Terahertz (THz) signals are not affected by FSO channel-related problems listed above (scintillation, low visibility in foggy conditions, Mie scattering effects, and high sensitivity to misalignment), but are highly impacted by other weather conditions, such as rain and snow. This suggests that the two transmission media (FSO and THz) can be operated in a complementary fashion, depending on the predominant weather and atmospheric conditions.

In this paper, we propose to use hybrid FSO-THz technology based on OAM to dramatically improve both spectral efficiencies and secrecy capacities of either RF/wireless or FSO links. It is well known that we can associate with a photon both spin angular momentum (SAM), related to polarization; and OAM, related to azimuthal dependence of the wavefront [14]. Because the OAM eigenstates are orthogonal, this additional degree of freedom can also be utilized to improve both spectral efficiency and physical-layer security in optical networks [3], [11]. On the hand, related to wireless communications, in series of papers, such as [15], [16], it has been shown that OAM can be generated in the RF domain as well, by employing circular array antennas, circular traveling-wave antennas, helical parabolic antennas, spiral phase plates, to mention few. Therefore, the key idea in this paper is to employ OAM in both FSO and THz subsystems to significantly improve the secrecy capacity, while ensuring that FSO and THz subsystems compensate for shortcoming of each other. Other spatial modes can also be used, however, the OAM modes require the lowest energies as the radial mode index is smallest. The THz technology is selected among various RF technologies, because the available bandwidths [17] are comparable to typical signal bandwidth per wavelength in WDM systems. To characterize the PLS, an information-theoretic definition of security is employed [18].

The contributions of the paper can be summarized as follows. The hybrid FSO-RF communications, have been considered before [19]. However, given that FSO channel bandwidth is orders of magnitude higher than that of RF channel, the improvements were moderate. By using properly selected THz technology, proposed here, as a subsystem with bandwidth comparable to a typical wavelength FSO channel, both spectral efficiency and PLS can be dramatically improved. Secondly, this is the first paper to study PLS of hybrid communication links. Thirdly, to

deal with atmospheric turbulence in FSO system either expensive adaptive optics approaches or multiple-input multiple-output (MIMO) signal processing approaches will be needed. In proposed multidimensional hybrid FSO-THz coded modulation, to improve the tolerance to atmospheric turbulence effects we need just to increase the dimensionality of the system as shown later in the paper. Fourthly, in FSO only systems in strong turbulence regime only small signal constellations can be transmitted. By using the proposed hybrid FSO-THz systems, even huge signal constellations can be transmitted over strong atmospheric turbulence channels. Finally, the hybrid FSO-THz system can support multi-Tb/s aggregate data rate transmission in the presence of strong atmospheric turbulence in FSO subsystem, which will quite challenging to achieve in FSO only system.

The paper is organized as follows. In Section 2, the proposed hybrid FSO-THz technology-based PLS and multidimensional coded modulation schemes are described, together with short description on generation/detection of OAM modes in both optical and RF domains. In Section 3, possible application scenarios of proposed hybrid FSO-THz communication systems are discussed. The relevant, illustrative, bit-error rate (BER) results for hybrid multidimensional coded modulation as well as secrecy capacity results for proposed PLC scheme are provided in Section 4. In Section 5, some important concluding remarks are provided.

2. Proposed Hybrid FSO-THz Coded Modulation and PLS Schemes

2.1. OAM Modes in Optical- and RF/THz-Domains

The angular momentum, J, of the classical electromagnetic field can be represented as [14]

$$\boldsymbol{J} = \frac{1}{4\pi c}\int_V \boldsymbol{E}\times\boldsymbol{A}\,dV + \frac{1}{4\pi c}\int_V \sum\nolimits_{k=x,y,z} E_k\,(\boldsymbol{r}\times\nabla)\,A_k dV, \tag{1}$$

where $\boldsymbol{E}$ is the electric field intensity, $\boldsymbol{A}$ is the vector potential, and c is the speed of light; wherein the vector $\boldsymbol{A}$ is related to the magnetic field $\boldsymbol{H}$ and electrical field $\boldsymbol{E}$ intensities by $\boldsymbol{H} = \nabla\times\boldsymbol{A}$ and $\boldsymbol{E} = -c^{-1}\partial\boldsymbol{A}/\partial t$, respectively. The second term in (1) is related to the OAM due to the presence of the angular momentum operator $\hat{\boldsymbol{L}} = -j(\boldsymbol{r}\times\nabla)$. Regarding the optical communications, among various optical beams that can carry OAM, the *Laguerre-Gaussian* (LG) vortex beams can easily be implemented with the help of spatial light modulators [14]. It has been shown in [14] (see also references therein) that different LG modes corresponding to a fixed *radial* index are all mutually orthogonal. The orthogonality principle is also satisfied for pure OAM basis functions, defined as $\phi_n = \exp(jn\phi)$; $n = 0, \pm1, \pm2, \cdots$, because

$$\langle\phi_m|\phi_n\rangle = \frac{1}{2\pi}\int_0^{2\pi} e^{-jm\phi}e^{jn\phi}d\phi = \begin{cases}1, & n=m\\ 0, & n\neq m\end{cases} = \delta_{nm} \tag{2}$$

Given that OAM-based basis functions are mutually orthogonal they can be used as the basis functions for either multidimensional signaling [1]–[3] or to improve the PLS in optical networks [11].

Regarding the generation of OAM modes for wireless applications, it has been recently shown that circular traveling-wave antenna, spiral parabolic antenna, dual mode antennas, and circular antenna arrays, to mention few, can be used to generate OAM modes in the RF domain [15], [16]. For instance, the circular traveling-wave antenna of radius a, with azimuthal dependence of current distribution $I = I_0 e^{jn\phi}$, based on [16], [20], will generate the electromagnetic (EM) waves with the

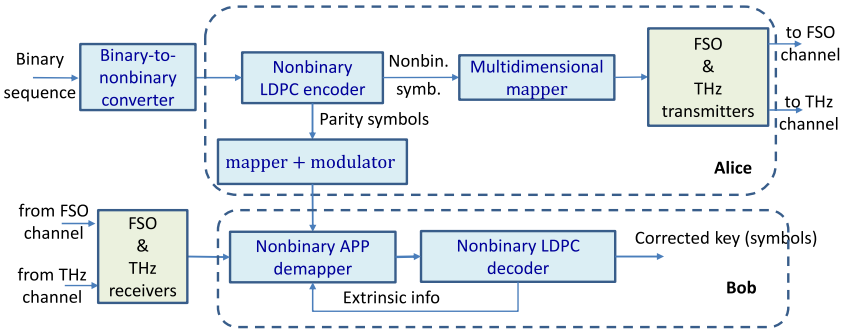

Fig. 1. Proposed hybrid FSO-THz PLS scheme.

vector potential expressed in spherical coordinates $[r, \theta, \phi]$ as:

$$\begin{aligned} \boldsymbol{A}(\boldsymbol{r}) &= \frac{\mu_0 I_0}{4\pi} \oint_L e^{jl\phi} \frac{e^{jk|\boldsymbol{r}-\boldsymbol{r}'|}}{|\boldsymbol{r}-\boldsymbol{r}'|} dl' \\ &\cong \frac{(-j)^{-n} a}{r} \frac{\mu_0 I_0 e^{jkr}}{4} e^{jn\phi} J_{n-1}(ka\sin\theta) \left[\sin\theta \hat{\boldsymbol{r}} + \cos\theta\hat{\theta} + j\hat{\phi}\right] \\ &+ \frac{(-j)^{-n} a}{r} \frac{\mu_0 I_0 e^{jkr}}{4} e^{jn\phi} J_{n+1}(ka\sin\theta) \left[\sin\theta \hat{\boldsymbol{r}} + \cos\theta\hat{\theta} - j\hat{\phi}\right]. \end{aligned} \tag{3}$$

Clearly, the term $e^{jn\phi}$ corresponds to the azimuthal phase dependence of the n-th OAM mode of the vector potential. After substitution of Eq. (3) into (1), because of the rotational symmetry only the angular momentum in the direction of propagation will survive the integration over the whole EM beam (wave), which can be expressed in cylindrical coordinates $[\rho, \phi, z]$ as follows:

$$L_z = \varepsilon_0 \int_0^{2\pi} d\phi \iint \mathrm{Re}\left\{j\boldsymbol{E}^* \left(\hat{\boldsymbol{L}} \cdot \boldsymbol{A}\right)\right\} \rho d\rho dz. \tag{4}$$

By segmenting this circular antenna into N segments, with each segment carrying the same RF signal but with an incremental phase shift of $2\pi n/N$, we can impose the n-th OAM mode on the RF carrier.

To detect a desired OAM mode in optical domain we need to use conjugate-complex computer generated hologram (CGH), recorded on SLM [14]. On the other hand, to detect a desired OAM mode in the RF/THz-domain, the corresponding segments in circular antenna need to be driven with incremental phase shits of opposite sign compared to that used on transmitter side. The RF/THz-domain OAM multiplexer/demultiplexer can be implemented with the help of multiple OAM antennas each imposing/detecting different OAM modes.

2.2. Description of Proposed Hybrid FSO-THz Technology-Based PLS Scheme

The proposed hybrid FSO-THz technology-based PLS scheme is provided in Fig. 1. The systematic nonbinary LDPC codes have been chosen because the information symbols stay intact while generalized parity-symbols are algebraically related to the information symbols. The information symbols are properly split and transmitted over the FSO and THz channels, as shown in Fig. 1, while the generalized parity symbols are transmitted over the authenticated classical channel. To improve the tolerance to atmospheric turbulence over FSO channel and multipath fading over THz channel, the multidimensional signaling is used. Given that FSO and THz channels have complementary properties, as discussed in Introduction, the probability of simultaneous FSO and THz channels' outage is very low.

The suitable operating wavelength of FSO subsystem is 1550 nm, while the suitable THz regions include 120 GHz and 250 GHz. In particular, 120 GHz technology is becoming commercially

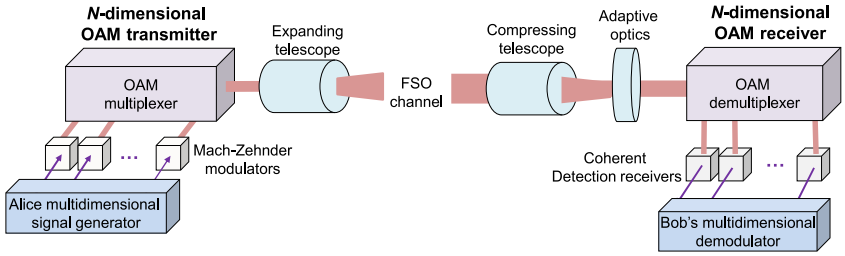

Fig. 2. The OAM-based FSO subsystem of proposed PLS scheme.

viable, while the distances longer than 5 km with data rates of 20 Gb/s have been reported [17], and as such represents an excellent THz technique to be used in proposed hybrid FSO-THz PLS scheme. Another relevant sub-THz (mm-wave) region, in particular for long-range distances is 85 GHz region with total atmospheric attenuation 0.5 dB/km [21]. To simplify the implementation, the initial multidimensional signal constellation is split into FSO and THz sub-constellations. On receiver side, after FSO and THz detection, the corresponding signals are converted into digital domain, and corresponding samples are passed to the nonbinary *a posteriori* probability (APP) demapper, where symbol log-likelihood ratios (LLRs) are calculated and passed to the corresponding LDPC decoder. The nonbinary LDPC coding is selected instead of binary coding to avoid the performance loss due to non-optimal mapping rules typically used in the literature. In particular, as shown in [1], the nonbinary LDPC coding over GF(4) represents a good compromise between complexity and performance.

In the proposed PLS scheme, the polarization state is not used for raw key transmission, but to detect the presence of Eve. After information reconciliation, the privacy amplification is then performed, to distill for the shorter key with negligible correlation with Eve. This key is then used for secure communication, based on one-time pad or any symmetric cipher. It is well-known that classical protocols rely on the computational difficulty of reversing the one-way functions, and in principle cannot provide any indication of Eve's presence. However, the FSO subsystem can be operated at a desired margin from the receiver sensitivity, and for known channel conditions the Eve's beam-splitting attack can be detected as it will cause sudden decrease in *secrecy capacity* C_s, defined as

$$C_s = C_{\mathrm{AB}} - C_{\mathrm{AE}}, \tag{5}$$

where C_{AB} is the instantaneous capacity of Alice-Bob channel and C_{AE} is the instantaneous capacity of Alice-Eve channel. From our recent studies of multidimensional signaling systems, such as [1]–[3]; we have learned that channel capacity can be increased linearly with number of degrees of freedom, rather than logarithmically with signal-to-noise ratio for conventional 2-D schemes. This observations motivates us to employ the OAM modes in both FSO and THz subsystems to dramatically improve secrecy capacity when compared to conventional 2-D schemes. The use of OAM modes to increase the secret key rates is always sensitive to the crosstalk among OAM modes and potential eavesdropper can compromise the security by relying on spatial coupling, without being detected by Alice and Bob. To solve for this problem, we propose to rely on multidimensional signaling. In *multidimensional signaling*, described in Section 2.3, the OAM modes are used as basis functions, and by detecting the signal in any particular OAM mode Eve will not be able to compromise security as only a single coordinate will be detected.

Before concluding this section, we provide additional details on FSO subsystem, which is shown in Fig. 2. Alice multidimensional signal generators provide the coordinates of sub-constellation corresponding to the FSO subsystem. The single transmit laser is used, whose output is split into N laser signals with the help of 1:N power splitter (optical star), and corresponding coordinates are imposed on the laser beam signals by Mach-Zehnder modulators (MZMs). Corresponding signals at MZMs' outputs are combined together by an OAM multiplexer, shown in Fig. 3(a), with corresponding OAM modes imposed with the help of CGHs. After optical amplification (by EDFA),

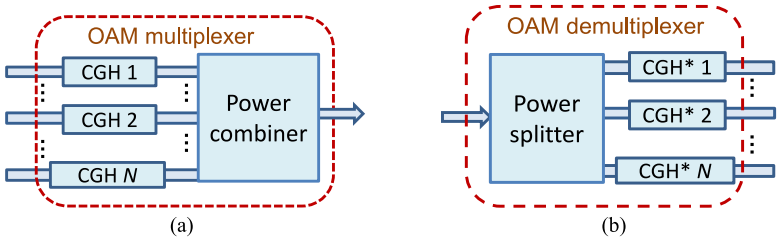

Fig. 3. Configuration of OAM: (a) multiplexer and (b) demultiplexer for FSO subsystem. CGH: computer generated hologram.

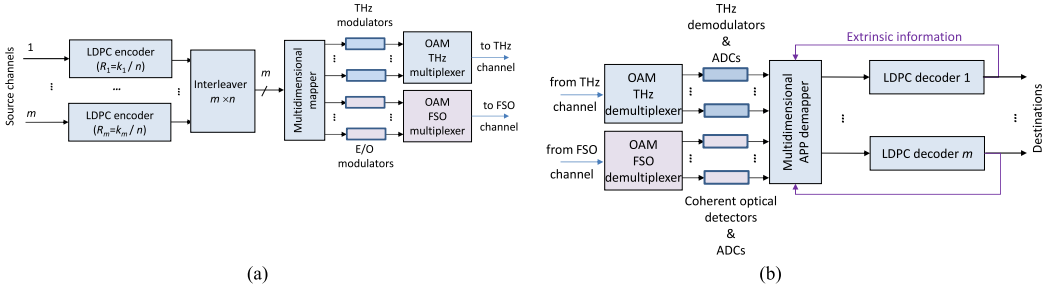

Fig. 4. Proposed hybrid FSO-THz multidimensional coded modulation scheme: (a) hybrid transmitter and (b) hybrid receiver configurations. E/O: electro optical modulator, ADC: analog-to-digital converter.

the multidimensional optical beam is transmitted by an expanded telescope towards the remote destination (Bob). The adaptive optics (AO) kit is used to reduce the distortions introduced by turbulence effects. The AO is optional, and it is not needed if FSO subsystem is used only in PLS. At Bob's side, the OAM demultiplexer, implemented as shown in Fig. 3(b), provides the projections along OAM basis functions, followed by the coherent optical detection. The same local laser is used to detect all OAM modes, with the help of 1:*N* power splitter (optical star). After coherent optical detection, the Bob's demodulator is able to determine the point transmitted in FSO sub-constellation.

2.3. Description of Proposed Hybrid FSO-THz Multidimensional Coded Modulation Scheme

The proposed hybrid FSO-THz multidimensional coded modulation scheme is shown in Fig. 4. This multidimensional coded modulation scheme belongs to the class of multilevel coding (MLC) with parallel independent decoding (PID) schemes [1]. The m independent data streams are (n_i,k_i) LDPC-coded, where k_i and n_i are information word length and codeword length, respectively, of the i-th data stream. The m bits are then taken from interleaver, designed in similar fashion as described in [22], and used to select a point in multidimensional signal constellation of size $M = 2^m$. The multidimensional mapper is implemented as a look-up-table (LUT) in which 2N-dimensional coordinates are stored, the first N corresponding to THz-subsystem and the last N to FSO-subsystem [see Fig. 4(a)]. In THz-subsystem, N one-dimensional THz modulators are used to impose the coordinates in THz-domain, and then corresponding coordinates are OAM multiplexed in corresponding multiplexer, by employing the principles described in Section 2.1. Alternatively, N/2 THz I/Q modulators can be used, combined with (N/2)-component OAM THz multiplexer. Such obtained THz OAM-multiplexed signal is directed towards the remote THz receiver. In FSO-subsystem, the last N coordinates are taken from multidimensional mapper, and converted into optical domain by N parallel electro-optical (E/O) modulators, such as MZMs. Alternatively, N/2 E/O I/Q modulators can be used, combined with (N/2)-component OAM FSO multiplexer. Corresponding coordinates in optical domain are then OAM multiplexed using the OAM multiplexer shown in Fig. 3(a). Such obtained OAM multiplexed signal is with the help of expanding telescope

projected towards the remote FSO receiver [see Fig. 4(a)]. The *2N*-dimensional hybrid FSO-THz modulator generates the signal constellation points as follows:

$$\boldsymbol{s}_i = \sum_{n=1}^{N} \psi_{i,n}^{(\mathrm{FSO})} \Psi_n^{(\mathrm{FSO})} + \sum_{n=1}^{N} \psi_{i,n}^{(\mathrm{THz})} \Psi_n^{(\mathrm{THz})}, \tag{6}$$

where $\psi_{i,n}^{(\mathrm{FSO})}$ [$\psi_{i,n}^{(\mathrm{THz})}$] denotes the n-th coordinate ($n = 1, 2, \ldots, N$) of the i-th signal-constellation point in FSO [THz] subsystem, and the set $\{\Psi_n^{(\mathrm{FSO})}\}$ [$\{\Psi_n^{(\mathrm{THz})}\}$] denotes the set of the OAM basis functions in FSO [THz] subsystem.

The hybrid receiver, shown in Fig. 4(b), is composed of THz and FSO receivers. In OAM THz demultiplexer, based on several OAM THz receiver antennas as described in Section 2.1, different projections along OAM THz modes are obtained. After that the THz demodulation takes place [23], with the help of *N* THz demodulators for each OAM projection, followed by analog-to-digital converters (ADCs). The corresponding samples are then forwarded to the multidimensional APP demapper. In FSO receiver, implemented as shown in Fig. 2, the size of incoming laser beam is compressed with the help of receive telescope, whose output is used as input to OAM demultiplexer, shown in Fig. 3(b), which provides the projections along optical OAM basis functions. Then *N* coherent optical detectors, sharing the same local laser as described in Section 2.2, are used to convert optical OAM projections into electrical domain, followed by ADCs. The samples at the output of ADCs, corresponding to FSO subsystem, are forwarded to the multidimensional APP demapper. The multidimensional symbol LLRs, for the proposed hybrid FSO-THz coded modulation scheme, are calculated as follows

$$LLR(\boldsymbol{s}_i) = -\frac{\sum_{n=1}^{N} \left| \boldsymbol{r}_n^{(\mathrm{FSO})} - \psi_{i,n}^{(\mathrm{FSO})} \right|^2}{2\sigma_{\mathrm{FSO}}^2} - \frac{\sum_{n=1}^{N} \left| \boldsymbol{r}_n^{(\mathrm{THz})} - \psi_{i,n}^{(\mathrm{THz})} \right|^2}{2\sigma_{\mathrm{THz}}^2}, \tag{7}$$

where we use $\boldsymbol{r}_n^{(\mathrm{FSO})}$ [$\boldsymbol{r}_n^{(\mathrm{THz})}$] to denote the n-th component of received signal constellation point $\boldsymbol{r}$ in FSO [THz] subsystem; while σ_{FSO}^2 [σ_{THz}^2] is the variance of an equivalent noise upon detection in FSO [THz] receiver. Clearly, even for large number of coordinates the symbol LLRs are easy to calculate for Gaussian noise dominated channels. After that bit LLRs are calculated in similar fashion as described in [1] and forwarded to *m* LDPC decoders [see Fig. 4(b)]. Once LDPC decoding process is completed, the extrinsic bit LLRs are calculated and used to calculate the prior symbol LLRs, which are used in multidimensional APP demapper to re-calculate the symbol LLRs, and this process constitutes the outer iteration. The LDPC decoder iterations are called here inner iterations. Additional details about iterative demapping and decoding in multidimensional coded modulation schemes can be found in [1]. The bits from several inputs can be combined together into nonbinary symbols, to solve for non-optimum mapping rule, and corresponding scheme can be referred to as nonbinary MLC scheme, with additional details provided in [1].

In the proposed hybrid FSO-THz coded modulation scheme, the polarization degrees of freedom is not used at all, since in corresponding PLS scheme the polarization state is used to monitor for Eve's presence. When polarization state is employed in hybrid coded modulation scheme, the data rate (spectral efficiency) can be doubled.

3. Possible Application Scenarios of Proposed Hybrid FSO-THz Communications Systems

In this section, we present a few envisioned applications of hybrid FSO-THz (mm-wave) systems, which are summarized in Fig. 5. These are by no means the only applications for this technology. As shown in Fig. 5(a), hybrid and FSO links will enable building future integrated software-defined network infrastructure (SDNI), capable of integrating ultra-high-throughput satellite (UHTS) networks, composite wireless infrastructures, heterogeneous networks (HetNets), hybrid networks,

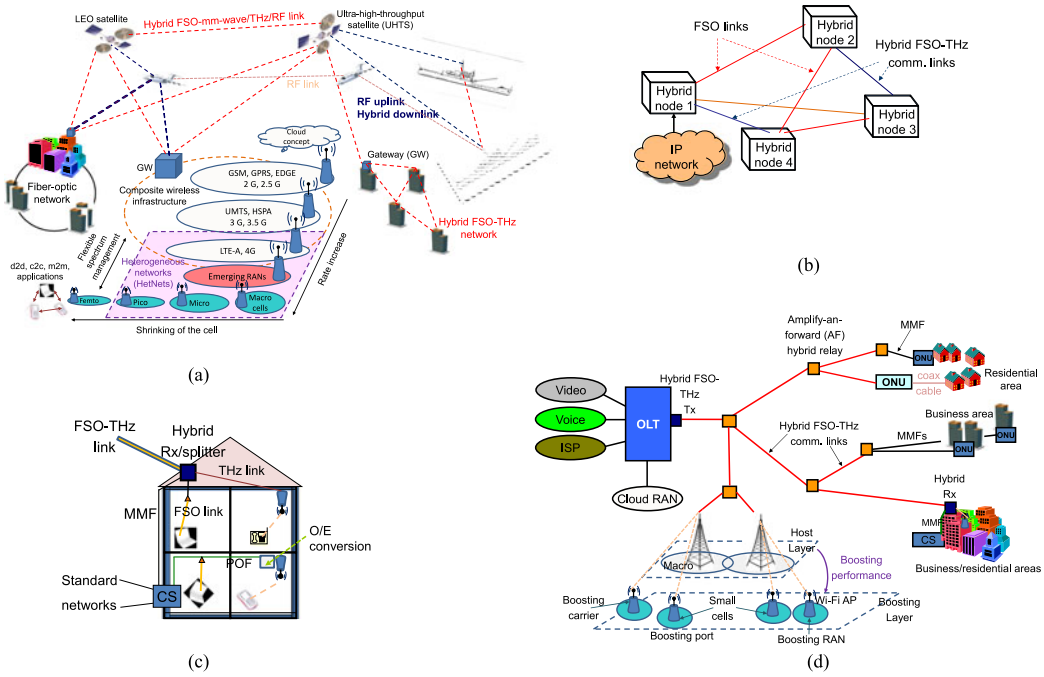

Fig. 5. Examples of hybrid FSO-THz/mm-wave/RF networks: (a) integrated hybrid communication enabled SDN infrastructure, (b) hybrid mesh-networking scenario, (c) indoor hybrid communications, (d) hybrid distribution/HetNet infrastructure. d2d: device-to-device, c2c: car-to-car, m2m: machine-to-machine.

fiber-optics networks, possible ship networks, to mention few. Hybrid links can be used as inter-satellite links (ISLs), and between LEO satellites and ground stations, UAVs, and ships.

The fiber-optic portion of the network could be a part of a MAN or WAN. Hybrid links can be used when fiber installation is expensive (e.g., in rural areas) or if it takes too much time to license and deploy (in urban areas). Satellites can serve as nodes in a mesh network, and ISLs can be established using FSO or hybrid links. In Fig. 5(b), we show an application of hybrid links in hybrid mesh networks, where hybrid nodes could be WiMAX routers, wireless mesh network (WMN) nodes, etc. The hybrid links can be used to enable ultra-high-speed access to residential/business buildings and homes, as illustrated in Fig. 5(c). We envision scenario in which signal is transmitted all way down to the PCs/laptops either all-optically or using THz technology, as illustrated in Fig. 5(c). In such scenario, the ceiling to PC/laptop link will be ether FSO link, such as IR or visible light communication (VLC) link, or THz link. The hybrid links can be used between the optical line terminal (OLT) of the ISP and the optical network unit (ONU), replacing SMF links, as shown in Fig. 5(d). Passive optical couplers, often used for this part of the optical network, would now be replaced by amplify-and-forward hybrid relays. ONU contains an optical receiver, together with the corresponding bandpass filter for downlink traffic and a laser for uplink traffic. For unicast and multicast applications, the ONU modules can be omitted. For WDM based solution, the OLT will contain a WDM laser array, external modulators corresponding to different wavelength channels, and WDM multiplexer for downlink traffic. For uplink traffic the TDM can be used, which requires maintaining the synchronization between ONUs. Alternatively, complementary wavelengths can be used for uplink traffic. However, such approach requires the use of increased number of wavelength channels for remote networks/ONUs. The cloud radio access networks (RANs) can be combined with the proposed distribution network as illustrated in Fig. 5(d). The data rate per each wavelength will be scalable to arbitrary high data rates by employing the OAM multiplexing/modulation principle. The superchannel OFDMA approach [1]–[3], which is compatible with SDN technology can also be employed in this scenario.

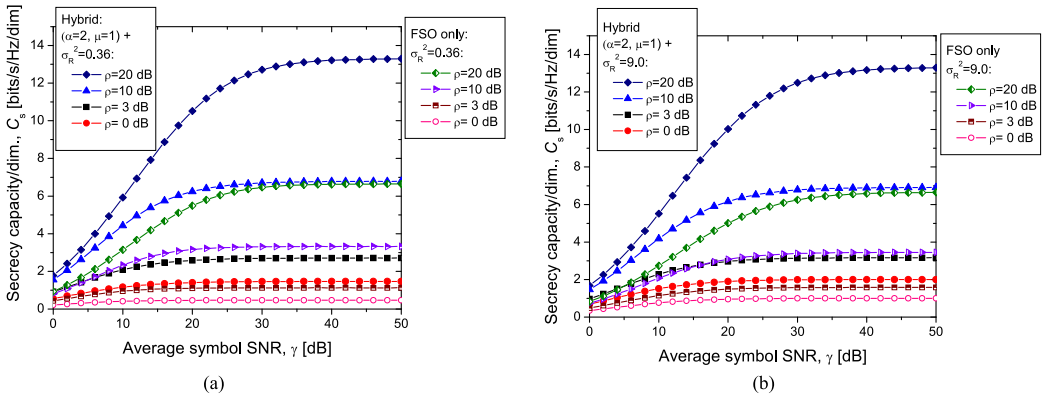

Fig. 6. Average hybrid FSO-THz secrecy capacities of proposed PLS scheme against FSO only secrecy capacities, for Rayleigh fading in THz subsystem.

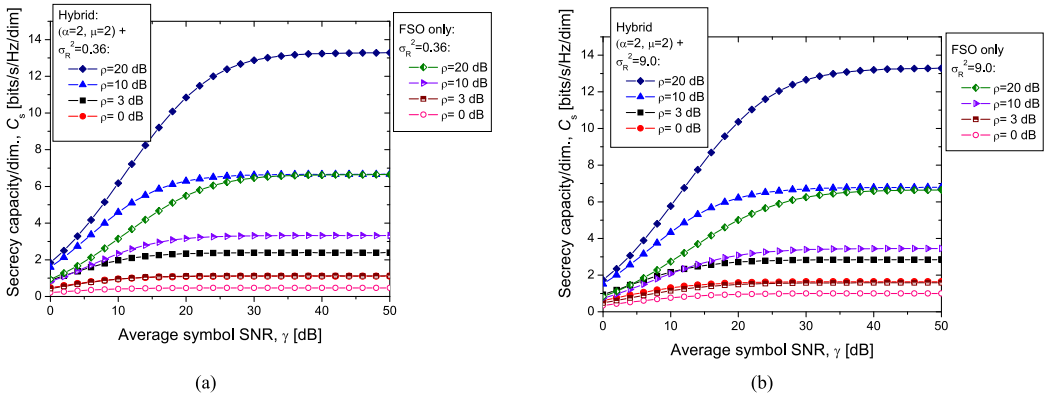

Fig. 7. Average hybrid FSO-THz secrecy capacities of proposed PLS scheme against FSO only secrecy capacities, for Nakagami-2 fading in THz subsystem.

4. Illustrative Secrecy Capacity Results and Coded Modulation BER Results

4.1. Secrecy Capacity Results of Proposed Hybrid PLS Scheme

To demonstrate high potential of the proposed hybrid FSO-PLS scheme, we perform the Monte Carlo simulations, with results of simulations summarized in Figs. 6–7. In each of the figures the ratio in average SNRs for Alice-Bob ($\bar{\gamma}_{AB}$) and Alice-Eve ($\bar{\gamma}_{AE}$) channels, defined as $\rho = \bar{\gamma}_{AB}/\bar{\gamma}_{AE}$, is used as a parameter. In Fig. 6, the secrecy capacities are provided, normalized per single dimension, of both hybrid FSO-THz system and FSO only system, which serves here as a referent case. The FSO channel is modelled by using gamma-gamma distribution [10]. The Rytov variance is used to characterize the turbulence strength, because it takes into account the operating wavelength λ, transmission distance L, and the refractive structure parameter C_n^2; and it is defined as $\sigma_R^2 = 1.23C_n^2(2\pi/\lambda)^{7/6}L^{11/6}$. Weak atmospheric turbulence is defined by $\sigma_R^2 < 1$, the moderate by $\sigma_R^2 \approx 1$, and the strong turbulence by $\sigma_R^2 > 1$. Evidently, when Eve is employing beam-splitting attack (with $\rho \approx 0$ dB) the turbulence strength helps improving the secrecy capacity. Moreover, with multidimensional signaling the secrecy capacity can be significantly improved compared to conventional 2-D schemes. The multipath THz fading channel is modelled by employing (α, μ)-distribution, which is chosen because Rayleigh, Nakagami-*m*, exponential, Weibull and one-sided Gaussian distribution functions, to mention few, are all special cases of α-μ distribution [24]. For instance, by setting $\alpha = 2$ and $\mu = 1$ we obtain the Rayleigh distribution, while by setting $\alpha = 2$ and $\mu = 2$ we obtain Nakagami $m = 2$ distribution. Since the Rayleigh distribution represents the worst-case scenario for the THz-subsystem, it has been employed in simulations in Fig. 6. Clearly, when the hybrid

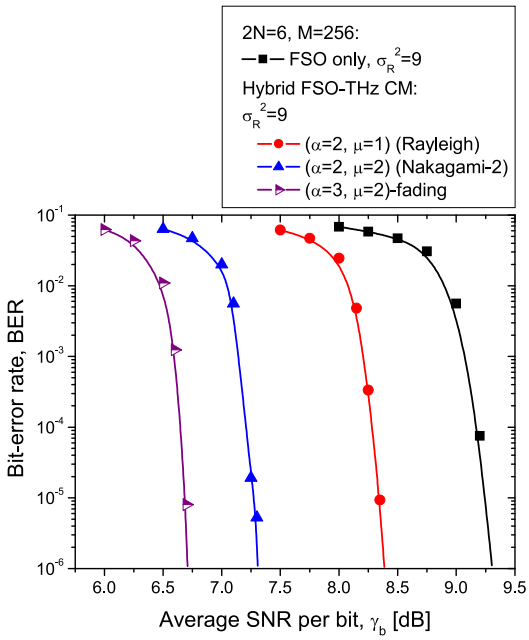

Fig. 8. BER performance of 256-ary 6-D hybrid FSO-THz LDPC (16935, 13550) coded modulation.

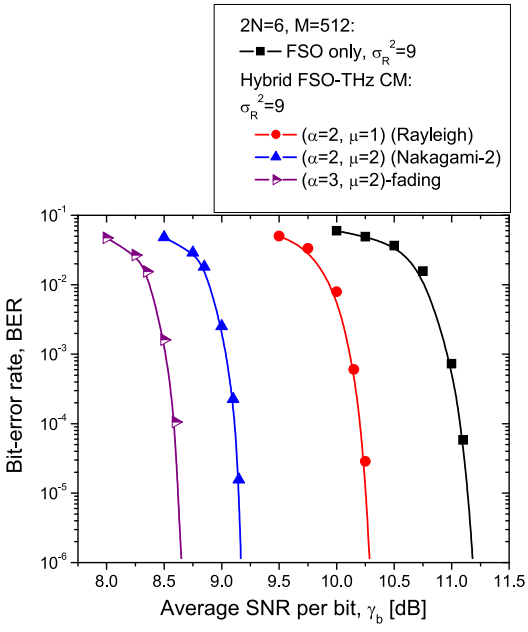

Fig. 9. BER performance of 512-ary 6-D hybrid FSO-THz LDPC (16935, 13550) coded modulation.

FSO-THz PLS scheme is used, the secrecy capacity of FSO system can be increased several times. For instance, in the weak turbulence regime, for SNR $=$ 20 dB, secrecy capacity can be increased 3.3 times for $\rho = 0$ dB. On the hand, for SNR $=$ 30 dB, the secrecy capacity of hybrid system is twice higher than that of FSO for $\rho = 20$ dB. In strong turbulence regime, the secrecy capacity for SNR $=$ 20 dB and $\rho = 0$ dB can be increased two times. Moreover, the hybrid system provides the robustness against atmospheric turbulence effects, given that results in weak and strong turbulence regimes, are not much different. As an illustration, for secrecy capacity per dimension of 4 bits/s/Hz and $\rho = 20$ dB, the hybrid system outperforms FSO system by 8.46 dB in strong turbulence regime.

Finally, the overall secrecy capacities of corresponding 2-D schemes can be increased $2N$ times by using the proposed hybrid FSO-THZ PLS scheme, employing N OAM modes in optical domain and N OAM modes in THz-domain.

In Fig. 7, the secrecy capacities (normalized per single THz and single FSO dimensions) are provided for hybrid FSO-THz PLS scheme, assuming Nakagami-2 fading in THz subsystem. The turbulence strength in FSO subsystem is again characterized by the Rytov variance. As expected, the improvements in secrecy capacities for hybrid system over FSO system for Nakagami-2 fading in THz subsystems are smaller than that for Rayleigh fading, given that Eve experiences less detrimental fading effects. For instance, the improvement in strong turbulence for $\rho = 0$ dB for hybrid system is 1.64 times higher than that of FSO, while the improvement for $\rho = 20$ dB is still twice higher. On the other hand, the tolerance to atmospheric turbulence effects is better for large ρ. For example, for secrecy capacity (per dimension) of 4 bits/s/Hz, with $\rho = 20$ dB, SNR tolerance of hybrid system over FSO system is 8.96 dB, which is slightly higher than that for Rayleigh fading in THz subsystem.

4.2. Illustrative BER Results for Proposed Hybrid FSO-THz Multidimensional Coded Modulation Scheme

Monte Carlo simulations for 256-ary and 512-ary six-dimensional (6-D, $2N = 6$) hybrid FSO-THz LDPC (16935, 13550) coded modulation (CM) are summarized in Figs. 8–9, respectively. Similarly, as in previous section, the FSO only system is used as a referent case. The LDPC code is a quasi-cyclic code of rate 0.8, with codeword length of 16935 and information word length of 13550. To reduce the complexity of MLC, the bit-interleaved coded modulation (BICM), in which all components code are identical, implemented as described in [22], is employed. In simulations it is assumed that channel state information is available on receiver side (CSIR scenario). The multidimensional signal constellations are obtained by employing the optimized vector-quantization-inspired signal constellation design (OVQ-SCD) [3]. It is also assumed that FSO channel is in strong turbulence regime, with Rytov variance of $\sigma_R^2 = 9$, to demonstrate high potential of the proposed hybrid coded modulation. Clearly, when there is no line-of-sight in THz channel, for Rayleigh fading, the performance of FSO only system can be significantly improved, by 0.93 dB at BER of 10^{-6} for 256-ary constellation.

When THz channel is Nakagami-2 fading, the BER performance are dramatically better than that of FSO only system, by more than 2 dB (at the same BER, for the same constellation). Finally, the improvement of hybrid system over FSO system, for ($\alpha = 3$, $\mu = 2$) fading in THz subsystem, is 2.59 dB (at BER of 10^{-6}).

The corresponding improvements for 512-ary constellation range from 0.9 dB in THz Rayleigh channel to 2.54 dB in ($\alpha = 3$, $\mu = 2$)-fading. What is interesting to notice is the fact that huge multidimensional signal constellations sizes, with high code rates LDPC codes, without MIMO signal processing, are applicable, which is not possible with conventional 2-D modulation schemes. With such large constellations, with commercial symbols rates (25 GS/s), it is possible to achieve multi-Tb/s aggregate data rates while operating FSO subsystem in strong turbulence, while such high data rates in FSO only systems are demonstrated only in a back-to-back configuration. For instance, by employing 512-ary 6-D constellation, with three THz and three FSO OAM states, with both polarization states, and both in-phase/quadrature channels, the aggregate data rate of 900 Gb/s is achieved even for small numbers of THz and FSO OAM states. Now by employing several wavelengths, the multi-Tb/s transmission over hybrid links would be possible.

5. Concluding Remarks

The proposed hybrid FSO-THz communication is a new frontier in high-speed communications, with potentially broad applicability in both commercial and defense networks. It promises several orders of magnitude increase in achievable transmission rates over state-of-the-art techniques and ensuring secure and uninterrupted operation irrespective of channel and weather conditions.

This paper has been concerned with PLS and high spectral efficiency of hybrid FSO-THz communication links. We proposed a hybrid PLS scheme composed of FSO and THz subsystems, compensating for shortcoming of each other. We have shown that the proposed PLS scheme can dramatically improve the secrecy capacity of corresponding 2-D scheme $2N$ times, by utilizing the N OAM modes in THz-domain and N OAM modes in optical-domain. We also proposed hybrid FSO-THz multidimensional coded modulation scheme exhibiting high tolerance to atmospheric turbulence effects. The proposed hybrid FSO-THz coded modulation significantly outperforms FSO only-based coded modulation in strong atmospheric turbulence regime, while enabling high spectral efficiency, even 16 bits/s/Hz, when both polarization states are employed.

References

[1] I. B. Djordjevic, "On advanced FEC and coded modulation for ultra-high-speed optical transmission," *IEEE Commun. Surv. Tuts.*, vol. 18, no. 3, pp. 1920–1951, Aug. 2016.

[2] I. B. Djordjevic, A. H. Saleh, and F. Küppers, "Design of DPSS based fiber Bragg gratings and their application in all-optical encryption, OCDMA, optical steganography, and orthogonal-division multiplexing," *Opt. Exp.*, vol. 22, no. 9, pp. 10882–10897, May 2014.

[3] I. B. Djordjevic, A. Jovanovic, Z. H. Peric, and T. Wang, "Multidimensional optical transport based on optimized vector-quantization-inspired signal constellation design," *IEEE Trans. Commun.*, vol. 62, no. 9, pp. 3262–3273, Sep. 2014.

[4] P. Demestichas *et al.*, "5G on the Horizon: Key challenges for the radio-access network," *IEEE Veh. Technol. Mag.*, vol. 8, no. 3, pp. 47–53, Sep. 2013.

[5] E. Hossain and M. Hasan, "5G cellular: Key enabling technologies and research challenges," *IEEE Instrum. Meas. Mag.*, vol. 18, no. 3, pp. 11–21, Jun. 2015.

[6] A. Hakiri and P. Berthou, "Leveraging SDN for the 5G Networks: Trends, prospects and challenges," in *Software Defined Mobile Networks: Beyond LTE Network Architecture* (Series in Communications Networking and Distributed Systems 2015). Hoboken, NJ, USA: Wiley, Jun. 2015, pp. 1–23.

[7] M. R. Palattella *et al.*, "Internet of things in the 5G Era: Enablers, architecture, and business models," *IEEE J. Sel. Areas Commun.*, vol. 34, no. 3, pp. 510–527, Mar. 2016.

[8] T. Rossi, M. De Sanctis, E. Cianca, C. Fragale, M. Ruggieri, and H. Fenech, "Future space-based communications infrastructures based on high throughput satellites and software defined networking," in *Proc. IEEE Int. Symp. Syst. Eng.*, Rome, Italy, 2015, pp. 332–337.

[9] L. Cheng, M. Zhu, M. M. U. Gul, X. Ma, and G.-K. Chang, "Adaptive photonics-aided coordinated multipoint transmissions for next-generation mobile fronthaul," *J. Lightw. Technol.*, vol. 32, no. 10, pp. 1907–1914, 2014.

[10] L. C. Andrews and R. L. Philips, *Laser Beam Propagation Through Random Media*. Bellingham, WA, USA: SPIE Press, 2005.

[11] X. Sun and I. B. Djordjevic, "Physical-layer security in orbital angular momentum multiplexing free-space optical communications," *IEEE Photon. J.*, vol. 8, no. 1, pp. 01110-1–01110-10, Feb. 2016.

[12] F. J. Lopez-Martinez, G. Gomez, and J. M. Garrido-Balsells, "Physical-layer security in free-space optical communications," *IEEE Photon. J.*, vol. 7, no. 2, Apr. 2015, Paper 7901014.

[13] A. D. Wyner, "The wire-tap channel," *Bell Syst. Tech. J.*, vol. 54, no. 8, pp. 1355–1387, Oct. 1975.

[14] I. B. Djordjevic and Z. Qu, "Coded orbital angular momentum modulation and multiplexing enabling ultra-high-speed free-space optical transmission," in *Optical Wireless Communications—An Emerging Technology*, M. Uysal *et al.*, Eds. New York, NY, USA: Springer, 2016, pp. 363–385.

[15] S. Zheng, X. Hui, X. Jin, H. Chi, and X. Zhang, "Transmission characteristics of a twisted radio wave based on circular traveling-wave antenna," *IEEE Trans. Antennas Propag.*, vol. 63, no. 4, pp. 1530–1536, Apr. 2015.

[16] A. Willner, Y. Yan, Y. Ren, N. Ahmed, and N. G. Xie, "Orbital Angular Momentum-based Wireless Communications: Designs and Implementations," in *Signal Processing for 5G: Algorithms and Implementations* F.-L. Luo and C. Zhang, Eds. pp. 296–318, Chichester, U.K.: Wiley.

[17] T. Nagatsuma, "THz communication systems," in *Proc. Opt. Fiber Commun.*, LA, CA, USA, Mar. 2017, Paper Tu3B.1.

[18] M. Bloch, J. Barros, M. R. D. Rodrigues, and S. W. McLaughlin, "Wireless information-theoretic security," *IEEE Trans. Inf. Theory*, vol. 54, no. 6, pp. 2515–2534, Jun. 2008.

[19] I. B. Djordjevic and G. T. Djordjevic, "On the communication over strong atmospheric turbulence channels by adaptive modulation and coding," *Opt. Exp.*, vol. 17, no. 20, pp. 18250–18262, Sep. 2009.

[20] C. A. Balanis, *Antenna Theory: Analysis and Design*, 4th Ed. Hoboken, NJ, USA: Wiley, 2016.

[21] A. V. Räisänen *et al.*, "Propagation at THz frequencies," in *Semiconductor Terahertz Technology: Devices and Systems at Room Temperature Operation* G. Carpintero, L. E. G. Munoz, H. L. Hartnagel, S. Preu, and A. V. Räisänen, Eds., Hoboken, NJ, USA: Wiley, 2015, pp. 160–211.

[22] D. Zou, C. Lin, and I. B. Djordjevic, "FPGA-based LDPC-coded APSK for optical communication systems," *Opt. Exp.*, vol. 25, no. 4, pp. 3133–3142, Feb. 2017.

[23] G. Carpintero, L. E. G. Munoz, H. L. Hartnagel, S. Preu, and A. V. Räisänen, *Semiconductor Terahertz Technology: Devices and Systems at Room Temperature Operation*. Chichester, U.K.: IEEE Press, 2015.

[24] M. D. Yacoub, "The α-μ distribution: A physical fading model for the Stacy distribution," *IEEE Trans. Veh. Technol.*, vol. 56, no. 1, pp. 27–34, Jan. 2007.